Journal of Intensive Medicine 5 (2025) 89–99

Contents lists available at ScienceDirect

Journal of Intensive Medicine

journal homepage: www.elsevier.com/locate/jointm

Original Article

Overexpression of Parkin promotes the protective effect of mitochondrial autophagy on the lung of rats with exertional heatstroke

Ran Meng[1,2], Zhengzhong Sun[1,2], Ruxue Chi[1,2], Yan Gu[2], Yuxiang Zhang[2], Jiaxing Wang[2,*]

[1] *Graduate School of Hebei North University, Zhangjiakou, Hebei, China*
[2] *Department of Critical Care Medicine, The Eighth Medical Center of Chinese PLA General Hospital, Beijing, China*

ARTICLE INFO

Managing Editor: Jingling Bao/Zhiyu Wang

Keywords:
Exertional heat stroke
Acute lung injury
Mitophagy
Pink1
Parkin

ABSTRACT

Background: The roles of the Pink1/Parkin pathway and mitophagy in lung injury during heat stroke remain unclear. In this study, we investigated the role of Pink1/Parkin-mediated mitophagy in acute lung injury (ALI) in rats with exertional heat stroke (EHS).

Methods: Sixty Sprague Dawley rats were randomly divided into control (CON), control + Parkin overexpression (CON + Parkin), EHS, and EHS + Parkin overexpression (EHS + Parkin) groups. Parkin was overexpressed by injecting an adeno-associated virus carrying the *Parkin* gene into the tail vein, and a rat model of EHS was established. Pathological changes in the lung tissue were analyzed using microcomputed tomography (micro-CT), and the lung coefficient and pulmonary capillary permeability were measured. Enzyme-linked immunosorbent assay were used to determine the levels of interleukin-6 (IL-6), IL-1β, and tumor necrosis factor-α, and reactive oxygen species. The morphology of mitochondria in type II epithelial cells of lung tissue was observed using transmission electron microscopy; and the apoptosis of lung tissue, the level of mitophagy, and the co-localization of Pink1 and Parkin were determined using immunofluorescence. The expression of Pink1, Parkin, mitofusin-2 (MFN2), phosphatase and tensin homolog (PTEN), PTEN-L, p62, and the autophagy marker microtubule-associated protein 1 light chain 3 (LC3) in rat lung tissue was measured by Western blotting, and the ratio of LC3II/LC3I was calculated.

Results: Compared with the EHS group, the survival rate of rats in the EHS + Parkin group was significantly higher. Their lung coefficient and pulmonary vascular permeability decreased and the pathological changes were significantly alleviated (P <0.05). Their levels of inflammatory factors and reactive oxygen species were significantly decreased (P <0.05), and the degree of mitochondrial swelling in pulmonary type II epithelial cells was alleviated. The apoptosis of lung tissue was alleviated, the colocalization of Pink1 and Parkin, LC3 and Tom20 was enhanced, and the ratio of LC3-II/LC3-I increased. The expression of Pink1, MFN2, PTEN-L, and p62 decreased, whereas the expression of PTEN was not significantly different from that in the EHS group (P >0.05).

Conclusion: Pink1/Parkin-mediated mitophagy dysfunction is one of the mechanisms underlying ALI in rats with EHS, and activation of Parkin overexpression-mediated mitophagy can alleviate ALI caused by EHS.

Introduction

Global warming is increasing the frequency and duration of extreme high-temperature weather and the annual incidence of heat stroke (HS).[1] HS is associated with high-temperature and high-humidity environments and has extremely high disability and mortality if not effectively treated. It is divided into “Classic HS” and “Exertional heat stroke (EHS)” according to the source of the heat.[2] EHS has a very high mortality and mostly occurs in individuals who work outdoors or train in the summer.[3] It is characterized by a core body temperature greater than 40 °C and is accompanied by central nervous system dysfunction, which progresses to mutipleorgan dysfunction in severe cases.[2] As an important organ regulating heat dissipation, the lung is vulnerable to heat stress, which leads to the occurrence of acute lung injury (ALI) or acute respiratory distress syndrome (ARDS).[4,5] Organ damage due to HS is associated with mitochondrial damage.[4] Mitochondria are important organelles in eukaryotic cells that are responsible for energy synthesis, metabolism, cell differentiation, and

* Corresponding author: Jiaxing Wang, Department of Critical Care Medicine, The Eighth Medical Center of Chinese PLA General Hospital, Beijing 10091, China.
E-mail address: wangjiaxing012@163.com (J. Wang).

https://doi.org/10.1016/j.jointm.2024.07.004
Received 23 April 2024; Received in revised form 2 July 2024; Accepted 29 July 2024
Available online 20 September 2024

apoptosis.[6] HS can directly cause mitochondrial damage and activate cell apoptosis.[6,7] Mitochondrial damage produces a large number of reactive oxygen species (ROS), enhances intracellular oxidative stress, and induces inflammation.[8] Oxidative stress and inflammatory reactions further disturb telomeres and damage mitochondria,[9] resulting in cascade amplification of oxidative stress, systemic inflammatory response syndrome (SIRS), and organ failure. Therefore, the effective and selective removal of damaged mitochondria is a crucial, adaptive response that supports the maintenance of human health.[10]

Mitophagy refers to the process whereby damaged, aging, and dysfunctional mitochondria are recognized by specific autophagosomes and selectively transported to lysosomes for degradation. It represents an important control that maintains mitochondrial quality and dynamic balance.[11] The Pink1/Parkin pathway is one of the classical pathways that regulate mitophagy. During sepsis, Parkin is transported from the cytoplasm to the mitochondria and induces mitophagy. In septic mice, *Pink1* and *Parkin* knockout resulted in more severe intracellular mitochondrial damage and higher levels of organ failure and mortality compared to controls.[12–15] However, the role of the Pink1/Parkin pathway and mitophagy in ALI during EHS remains unclear. Mitochondrial damage and SIRS occur in EHS owing to its pathophysiological mechanism being similar to that of sepsis. In this study, we established the EHS rat model to observe the effect of Parkin overexpression on the lung tissue and explore the role of the Pink1/Parkin pathway in EHS-induced lung injury. Our results provide a theoretical basis for the treatment of ALI by EHS.

Methods

Animals

Sixty healthy male 8-week-old Sprague Dawley rats, weighing 300 g–350 g were purchased from Home-SPF (Beijing Biotechnology Co., Ltd.; License number: SCXK [Beijing] 2019–0010). The animals were raised in the animal laboratory under specific pathogen-free conditions, moderate ventilation, a 12-h light/dark cycle, at 25 ˚C–26 ˚C, and relative humidity of 50 %–60 %. The animal experimentation was approved by the Animal Ethics Committee of the 8th Medical Center of Chinese PLA General Hospital (approval number: 20208141030).

Antibodies used

Anti-rat glyceraldehyde phosphate dehydrogenase (GAPDH) monoclonal antibody, rabbit anti-rat p62, mouse anti-rat Tom20, rabbit anti-rat Pink1 polyclonal antibodies, and rabbit anti-rat mitofusin-2 (MFN2) polyclonal antibodies were purchased from Abcam (Cambridge, UK); rabbit anti-rat microtubule-associated protein 1 light chain 3 (LC3) polyclonal antibody, mouse anti-rat Parkin monoclonal antibody, and mouse anti-rat phosphatase and tensin homolog (PTEN) polyclonal antibody were purchased from Cell Signaling Technology (Danvers, MA, USA); mouse anti-rat PTEN-α monoclonal antibody was purchased from Merck Millipore (Burlington, MA, USA); and horseradish peroxidase-labeled goat anti-rabbit polyclonal antibody was purchased from Beijing ZSGB-BIO Biotechnology Co., Ltd (China).

Animal groups and model construction

The rats were randomly divided into four groups: control (CON), control + Parkin overexpression (CON + Parkin), EHS, and EHS + Parkin overexpression (EHS + Parkin) groups; with 15 rats in each group. Before HS modeling, all the experimental rats were placed into a transparent simulated high-temperature and humidity environment experimental cabin containing a six-track small animal treadmill (XR-PT-10A; Shanghai Xin Ruan Information Technology Co., Ltd., Shanghai, China). After 7 days of adaptive feeding in both the CON + Parkin and the EHS + Parkin rats, 300×10^{-9} L of an adeno-associated virus carrying the *Parkin* gene (OBiO Technology, Shanghai, China) was injected into the tail vein to overexpress Parkin in the lung tissues.[16] Four weeks after injection, the heat stress experiments were performed in both the EHS and the EHS + Parkin rats. Prior to the experiment, the rats were fasted for 12 h and provided with unlimited drinking water. Thirty minutes before the start of the modeling, the rats were weighed and drinking water was removed, stimulating defecation. When the temperature of the experimental cabin reached (39.5±0.3) ˚C and the relative humidity was (55±5)%, the rats were placed onto the treadmill, which was started at an initial speed of 5 m/min (slope=0).[17] The speed was increased by 1 m/min every 2 min. After 20 min, the speed was increased to 15 m/min, maintained until fatigue occurred, and then stopped. Consciousness and mental changes in the rats were closely observed throughout the experiment. The diagnostic criterion for EHS is central nervous system dysfunction; for example, a duration of no autonomic activity for more than 5 s (mild painless stimulation does not cause animals to crawl or change position).[17] Once the rats reached the diagnostic criterion of EHS, heat exposure was stopped by removal from the hot chamber. The rats were weighed, cooled naturally at 24˚C–26˚C, and their mental state was monitored until 5 h after modeling. Both the CON and the CON + Parkin rats were placed in the experimental cabin (temperature [25±0.3]˚C, relative humidity [30±5]%). Neither group was subjected to heat stress or running stimulation. After 1 h, the rats were removed and observed at room temperature for 5 h.

Measurement of the core body temperature within 3 h of modeling

After the rats were modeled, the anal temperature meter was calibrated, and an anal temperature sensor was coated with lubricant and inserted horizontally into the anus at a depth of 5–7 cm. The core body temperature was maintained for 10 s before the measurement was recorded every 10 min for 3 h. The core body temperature curve for each group was then generated.

Calculation of the 5-h survival rate

Fifteen rats in each group were observed and recorded at 0, 1, 2, 3, 4, and 5 h after modeling, and survival curves were constructed to calculate the survival rate of each group.

Rat lung microcomputed tomography (micro-CT)

Five hours after modeling, the rats were anesthetized by isoflurane inhalation, and images of the rat lungs were recorded

using a micro-CT instrument. The measurement parameters were: photographing time, 120 s; voltage, 90 kV; current, 160 μA; and photo pixel, 40 μm.

Histopathological analysis of rat lungs

Small pieces of tissue from the lower lobe of the right lung were dissected and fixed. The sections were dehydrated, embedded in paraffin, sectioned (5 μm), dewaxed, stained with hematoxylin and eosin, and the pathological changes in the lung tissue observed under a DM4000B optical microscope (Leica instrument Co., Ltd., Knokke-Heist, Belgium) at 200× magnification. Ten visual fields were randomly selected, and the pathological injury score of the lung tissue was evaluated as described by Hong et al.[18] The average was then calculated. In addition, the degree of pulmonary interstitial and alveolar edema was scored as 0, 1, 2, and 3 and the average score was calculated.[19]

Measurement of pulmonary vascular permeability

The Evans blue (EB) dye exudation technique was used to determine the lung tissue permeability.[20] EB (MedChemExpress, Monmouth Junction, NJ, USA) was dissolved in 2 % normal saline and injected into the tail vein of rats at a dose of 2 mL/kg. The ears and eyes of the rats turned blue, confirming that the EB dye was uniformly distributed in the rats. The EB dye was circulated *in vivo* for 2 h, and the abdominal cavity was anesthetized. After thoracotomy, the right atrial appendage was cut, and the pulmonary circulation was flushed through the left ventricle with 10 mL of phosphate buffer saline (PBS). The lung tissue was soaked in formamide (Shanghai Macklin Biotechnology Co., Ltd., Shanghai, China) solution and then incubated with formamide at 60°C for 16 h. Once all the pigment was extracted, the tissue was removed. After centrifugation at 7000 × *g* for 10 min, the supernatant was collected and the absorbance was measured to calculate the EB content of the tissue.

Determination of the lung coefficient

The rats were sacrificed by abdominal aortic bloodletting, and the lung tissues were collected and rinsed repeatedly with PBS. The surface water was removed with filter paper, the lungs were weighed, and the lung coefficient (lung weight/body weight [LW/BW]) was calculated. LW/BW = wet LW (mg)/rat BW (g).

Enzyme-linked immunosorbent assay (ELISA)

The levels of cytokines interleukin (IL-6), IL-1β, and tumor necrosis factor-α (TNF-α) and ROS in the lung tissues were determined by double-antibody sandwich ELISA using the Rat IL-6, IL-1β, TNF-α (Abcam) and ROS (Shanghai Yaji Biotechnology Co., Ltd., Shanghai, China) ELISA kits, according to the manufacturer's instructions.

Transmission electron microscopy

The tissue mass of the left lower lung of the rats, approximately 1 mm^3, was fixed with 2.5 % glutaraldehyde solution and rinsed with PBS three times for 15 min each. The tissue was then fixed with 1 % osmic acid for 2 h and then rinsed three times with PBS. Ethanol gradient dehydration, embedding, and polymerization were used to create a resin block, which was later sectioned on an ultrathin microtome and double-stained with 3 % uranyl acetate-lead citrate. The section, supported on a copper mesh, was viewed and analyzed using a JEM-1230 transmission electron microscope (Jeol Ltd., Tokyo, Japan) at 30,000× magnification.

TdT-mediated dUTP nick-end labeling (TUNEL)

The lung paraffin sections were dewaxed with gradient ethanol, rinsed with tap water, dripped into the working solution of protease, incubated at 37 °C for 20 min, and washed with PBS. The TUNEL solution (Hoffmann-La Roche Co., Ltd. Basel, Switzerland) was then added and incubated at 37 °C for 1 h. After washing with PBS, TUNEL solution was added and incubated at 24 °C–26 °C for 20 min. After washing with PBS, the sections were stained with diaminobenzidine and hematoxylin before gradient ethanol dehydration. The sections were then mounted and observed under a light microscope. ImageJ (Developed by National Institutes of Health) software was used for analysis.[21] Five visual fields were randomly selected under the microscope and the apoptosis index was calculated. Apoptosis index (%) = (number of positive cells/total number of cells) × 100.

Western blotting method and calculation of the LC3II/LC3I ratio

Protein was extracted from a fresh right upper lung tissue sample using 1 mL of radioimmunoprecipitation assay buffer, and the concentration was determined using a bicinchoninic acid kit. The protein samples were then separated using sodium dodecyl sulfate-polyacrylamide gel electrophoresis and transferred to a membrane by electroblotting. The antibody working solution was prepared according to the manufacturer's instructions. Pink1, Parkin, p62, and LC3 antibodies were all diluted at 1:2000. The membrane was blocked with skimmed milk powder solution, and the primary antibodies were incubated at 4 °C on a shaker overnight. The corresponding secondary antibodies (1:5000) were incubated at 24 °C–26 °C for 1 h and the results were visualized by enhanced chemiluminescence. The optical density of the bands was analyzed using ImagePro Plus 6.0 (Media Cybernetics, Rockville, MD, USA), and the relative expression was calculated as the ratio of the absorbance of the bands to that of the GAPDH internal reference.

Immunofluorescence detection

Paraffin sections of rat lung tissues were dewaxed with gradient ethanol, dehydrated, dried, and then washed with PBS three times before fixing at 24 °C–26 °C for 1 h with 1 % Triton X-100 and 2 % sheep serum. After washing in PBS, the sections were incubated with Pink1 (1:50), Parkin (1:50), LC3 (1:50), and Tom20 (1:100) primary antibodies at 4 °C overnight. After washing, DyLight 594-labeled goat anti-rabbit or DyLight 488-labeled goat anti-mouse secondary antibodies were added and incubated at 24 °C–26 °C for 30 min. After washing with PBS,

the nucleus was stained with 4′,6-diamidino-2-phenylindole. Co-staining of Pink1 and Parkin, LC3, and Tom20 in the lung tissue was observed using Olympus FV3000 confocal microscopy (Tokyo, Japan).

Statistical analysis

GraphPad Prism 9 software (GraphPad Software, Boston, MA, USA) was used for statistical analysis. The data are expressed by mean ± standard deviation. One-way analysis of variance was used for comparison among groups, and the Student–Newman–Keuls-*q* test was used for comparison between groups. Differences were considered statistically significant at P <0.05.

Results

Comparison of core body temperature changes in each group

The core body temperatures of the CON and CON + Parkin groups were maintained at approximately 37 ˚C–38 ˚C, whereas those of the EHS rats increased sharply and reached 43 ˚C. After exiting the thermal environment, the core body temperature of the EHS group decreased gradually, between 100 min and 125 min, the core body temperature was lower than that of the CON group. Compared to the EHS group, the core body temperature of the EHS + Parkin group remained stable after reaching normal body temperature (Figure 1).

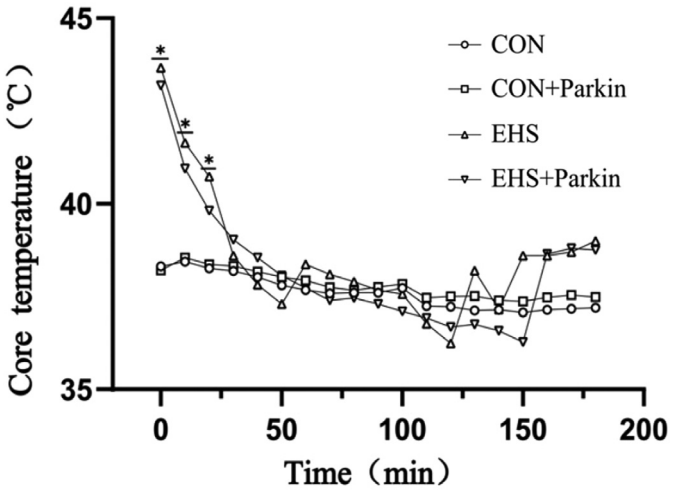

Figure 1. Changes in the core body temperature in each group.
*P <0.001 *vs.* CON group. n=5.
CON: Control; EHS: Exertional heat stroke.

The effect of Parkin overexpression on survival in EHS rats

The 1, 3, and 5 h survival rates of the EHS group after heat shock were approximately 86.7 % (13/15), 53.3 % (8/15), and 33.3 % (5/15), respectively (Figure 2). Compared to the EHS group, the survival rates of the EHS + Parkin group were significantly higher (P <0.05), except at 2 h where it was similar. There was no difference in the survival rates of rats in the CON and CON + Parkin groups.

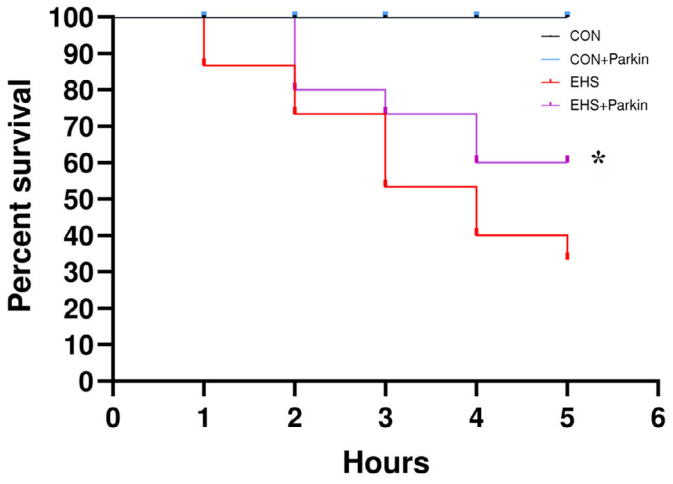

Figure 2. Survival rate of the experimental groups.
*P <0.05 *vs.* EHS group. n=15
CON: Control; EHS: Exertional heat stroke.

The effect of Parkin overexpression on pulmonary micro-CT imaging in EHS rats

Micro-CT showed patchy exudation and increased texture in the lung tissues of the EHS group (Figure 3). In the EHS + Parkin group, the patchy exudation of both lungs was significantly decreased and the texture was slightly increased compared to the EHS group (P <0.05). There were no significant differences observed between the CON and CON + Parkin groups.

Effect of Parkin overexpression on the lung coefficient and pulmonary vascular permeability in EHS rats

Figure 4 shows that the lung coefficient (Figure 4A) and pulmonary vascular permeability (Figure 4B and C) of the EHS group were significantly higher than those in the CON group (P <0.001). In contrast, the lung coefficient (Figure 4A) and pulmonary vascular permeability (Figure 4B and C) of the EHS + Parkin group decreased significantly compared with those of the EHS group (P <0.05). There was no significant difference in lung coefficient and pulmonary vascular permeability between the CON and CON + Parkin groups (P >0.05).

Parkin overexpression causes rats to resist the EHS-induced pathological changes in the lung

The lung tissue structures of the CON and CON + Parkin groups were clear, the alveolar wall was smooth, and no fluid exudation was observed in the alveolar cavity (Figure 5A). In the EHS group, a large number of red blood cells, inflammatory cells, and plasma-like substances were present in the alveolar cavity (Figure 5A); and the pulmonary pathology score (Figure 5B) and pulmonary edema scores (Figure 5C) increased significantly (P <0.001). Compared to the EHS group, alveolar collapse, inflammatory infiltration, pulmonary pathology score,

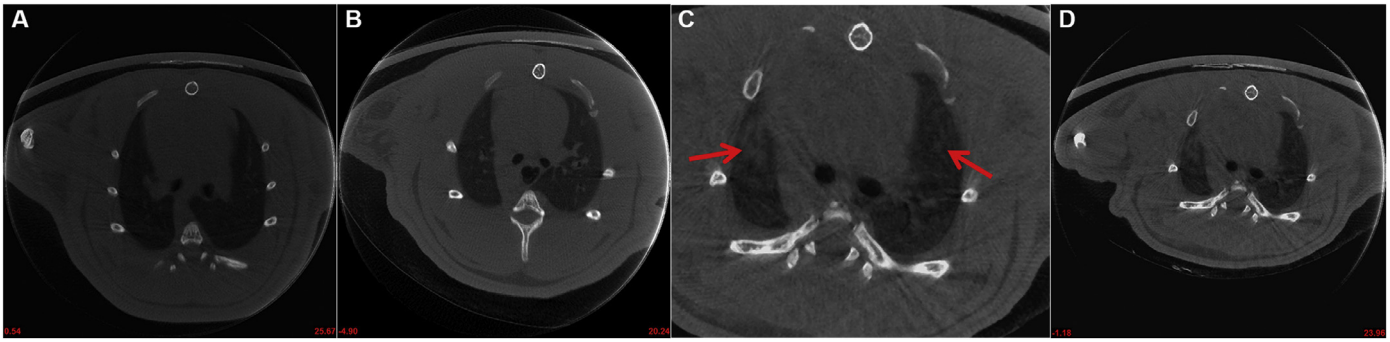

Figure 3. Parkin overexpression attenuates lung injury in EHS rats. Micro-CT images of representative lung scans of four froups. A: CON group. B: CON + Parkin group. C EHS group, Red arrows denote patchy exudation. D: EHS + Parkin group.
CON: Control; EHS: Exertional heat stroke; micro-CT: Microcomputed tomography.

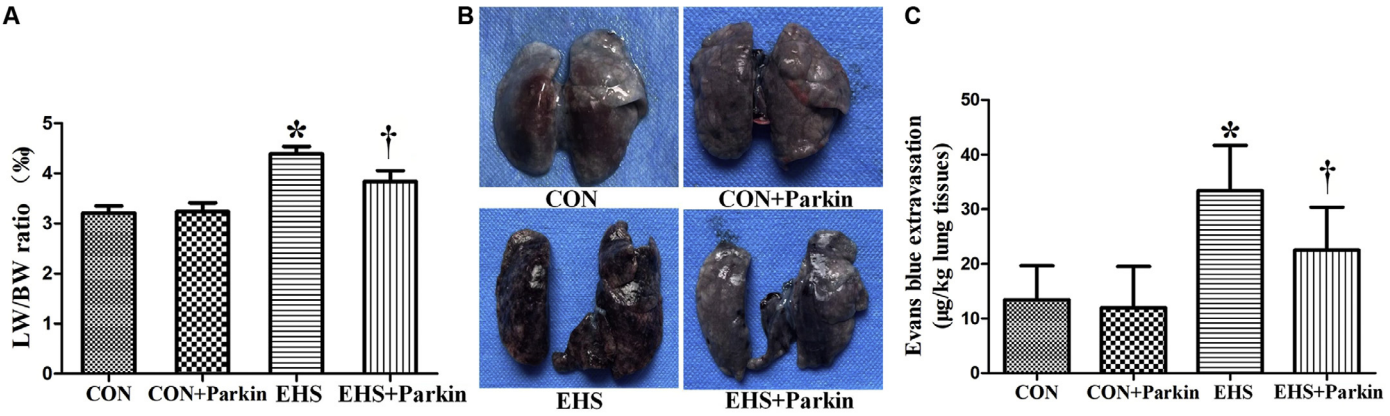

Figure 4. The overexpression of Parkin decreased the pulmonary index and vascular permeability of EHS rats. A: Pulmonary index. B: EB staining of lung tissue. C: Measurement of the pulmonary vascular permeability.
*P <0.001 *vs.* CON group;
†P <0.05 *vs.* EHS group.
CON: n=15; CON + Parkin: n=15; EHS: n=5; EHS + Parkin: n=9.
BW: Body weight; CON: Control; EB: Evans blue; EHS: Exertional heat stroke; HS: Heat stroke; LW: Lung weight.

and pulmonary edema score were significantly lower (P <0.05) in the EHS + Parkin group (Figure 5).

Effect of Parkin overexpression on the levels of IL-6, IL-1β, TNF-α, and ROS in the lung

Figure 6 shows that the levels of IL-6, IL-1β, TNF-α, and ROS in the lung tissues of the EHS group were significantly increased compared with those in the CON group (P <0.001), whereas their levels in the EHS + Parkin group were significantly lower than those of the EHS group (P<0.05). There were no significant differences in cytokine levels between the CON and CON + Parkin groups (P >0.05).

Morphologically, pulmonary mitochondrial injury was attenuated to a greater extent in EHS + Parkin rats

Transmission electron microscopy revealed that the morphology of mitochondria in type II lung epithelial cells of rats in the CON and CON + Parkin groups was regular, and the arrangement of the mitochondrial crest was compact and could be seen clearly (Figure 7A and B). In the EHS group, the mitochondria were swollen, the mitochondrial cristae were broken, and most mitochondria were vacuolated (Figure 7C), whereas in the EHS + Parkin group, the volume of mitochondria increased slightly, the degree of mitochondrial swelling was lower than that in the EHS group, the mitochondrial crest was intact, and there was no vacuolization (Figure 7D).

Pulmonary apoptosis was attenuated in the EHS + Parkin group

Figure 8 shows that the number of apoptotic cells (Figure 8A) and the apoptotic index (Figure 8B) in the lung tissue of the EHS group were significantly higher than those in the CON group (P <0.001); and in the EHS + Parkin group, they were significantly lower than the EHS group (P <0.05). There was no significant difference in lung tissue apoptosis between the CON and CON + Parkin groups.

Effect of Parkin overexpression on mitophagy levels in lung tissues

The expression of Parkin in the lung tissue of the CON + Parkin and EHS + Parkin groups increased after intravenous injection of an adeno-associated virus carrying the *Parkin* gene (Figure 9A). In the lung tissue of the EHS group, the expression of Parkin was increased (P <0.001), the autophagy

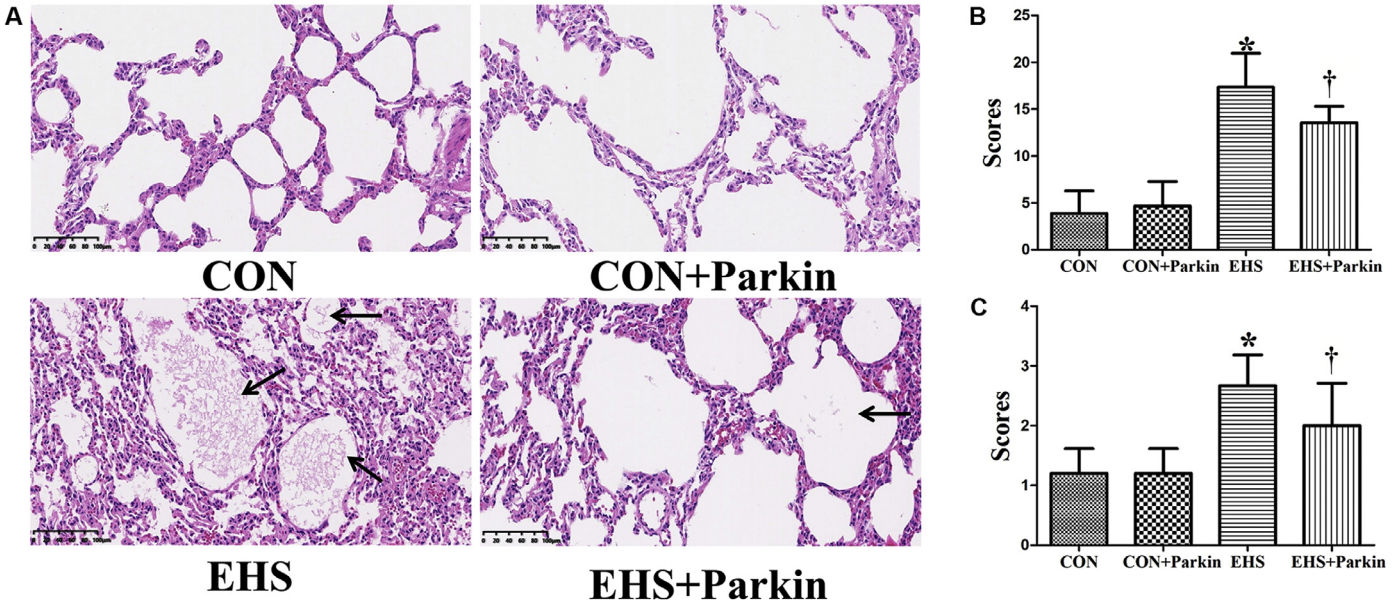

Figure 5. Histopathological analysis of the lungs (hematoxylin and eosin staining). A: The pathological changes of the lung in each group of rats. Arrows indicate the exudation in the alveolar cavity. Scale bar = 100 μm. B: Pulmonary pathology scores. C: Pulmonary edema scores.
*P <0.001 *vs.* CON group;
†P <0.05 *vs.* EHS group.
CON: n=15; CON + Parkin: n=15; EHS: n=5; EHS + Parkin: n=9.
CON: Control; EHS: Exertional heat stroke.

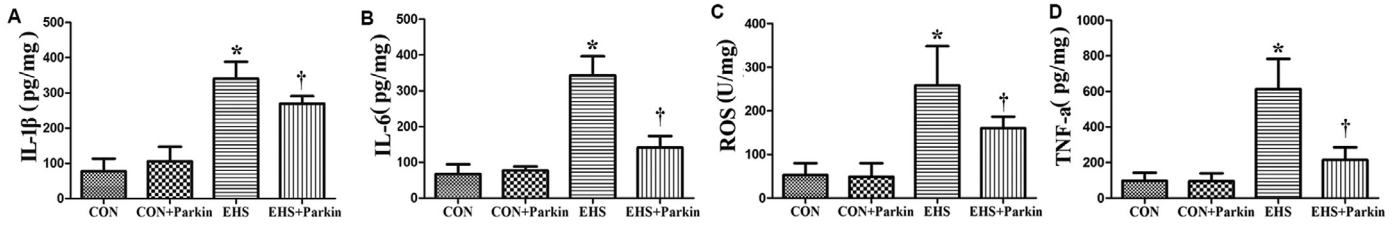

Figure 6. Parkin overexpression attenuates the EHS-induced increase in IL-1β, IL-6, TNF-α, and ROS in the lung. A: IL-1β. B: IL-6. C: ROS. D: TNF-α.
*P <0.001 *vs.* CON group;
†P <0.05 *vs.* EHS group.
CON: n=15; CON + Parkin: n=15; EHS: n=5; EHS + Parkin: n=9.
CON: Control; EHS: Exertional heat stroke; IL: Interleukin; ROS: Reactive oxygen species; TNF-α: Tumor necrosis factor-α.

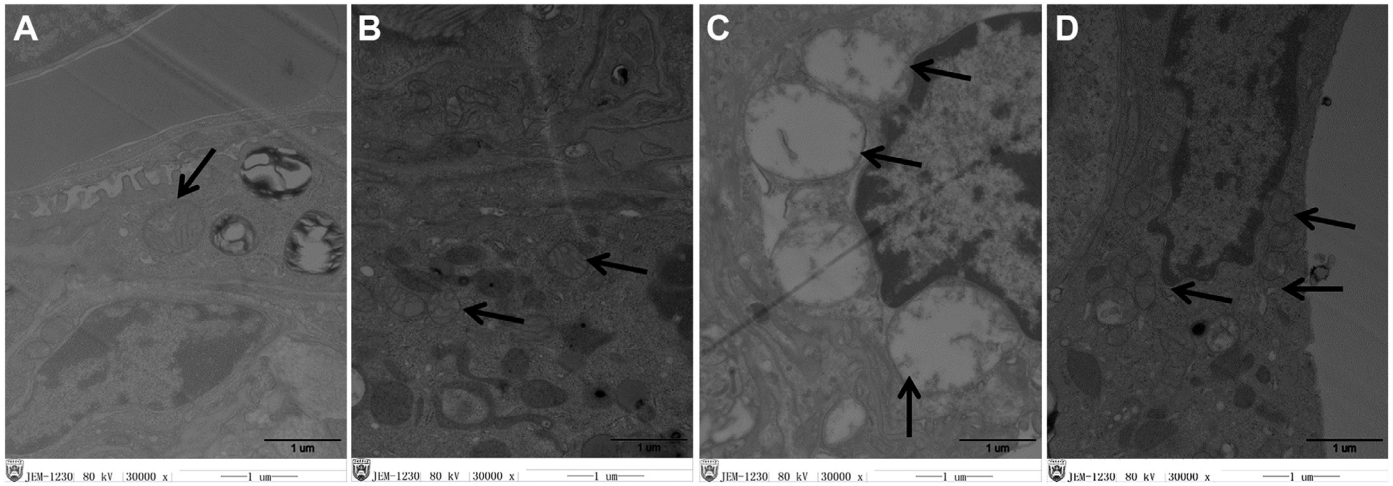

Figure 7. Mitochondrial morphology in lung epithelial cells. A: CON group. B:CON + Parkin group.C: EHS group. D: EHS + Parkin group. Arrows indicate mitochondria. Scale bar = 1 μm.
CON: Control; EHS: Exertional heat stroke.

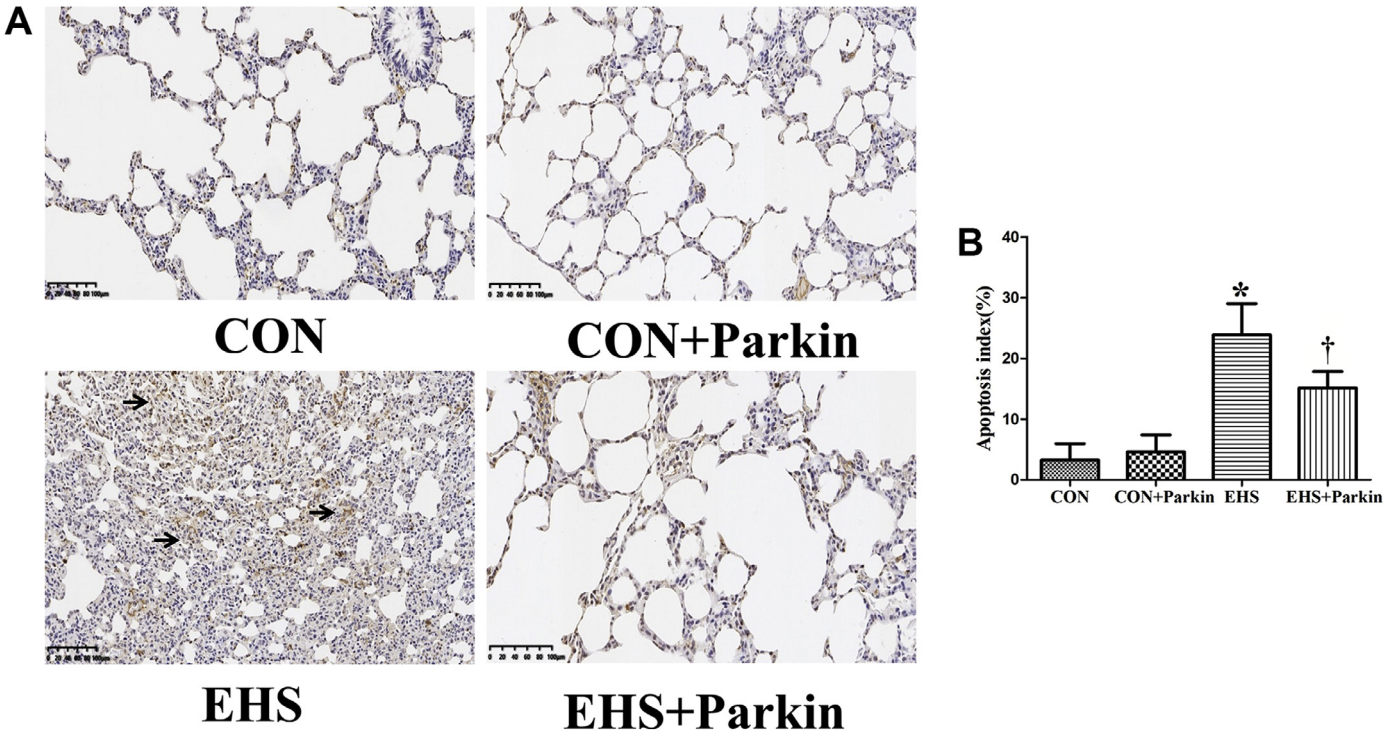

Figure 8. The effect of Parkin overexpression on apoptosis in lung tissue. A: TUNEL staining of the lung in each group of rats. Apoptotic cells are stained brown, whereas normal cells are stained blue. Scale bar = 100 μm. B: Apoptosis index.
*P <0.001 *vs.* CON group;
†P <0.05 *vs.* EHS group.
CON: n=15; CON + Parkin: n=15; EHS: n=5; EHS + Parkin: n=9.
CON: Control; EHS: Exertional heat stroke; TUNEL: TdT-mediated dUTP nick-end labeling.

level marker LC3-II/LC3-I ratio was significantly decreased (P <0.001), and the expression of p62 was increased (P <0.001) compared to the CON group (Figure 9B–D). In the EHS + Parkin group, the LC3-II/LC3-I ratio was elevated (P <0.05) and the expression of p62 was reduced (P <0.05) compared to the EHS group.

Compared with the CON group, the fluorescence intensity of LC3 (green) in the lung tissue of the EHS group was decreased and the colocalization (orange) fluorescence intensity of LC3 (green) and Tom20 (red) was also decreased (Figure 9E). In the EHS + Parkin group, the fluorescence intensity of LC3 and colocalization of LC3 and Tom20 were higher than in the EHS group. The ratio of LC3-II/LC3-I in the CON + Parkin group was slightly higher than that in the CON group; however, there was no difference in the expression of p62. The fluorescence intensity of LC3 and the colocalization of LC3 and Tom20 were also enhanced.

Parkin overexpression activates the Pink1/Parkin pathway in the lung tissue of EHS rats

Western blotting showed that the expression of Pink1, Parkin, MFN2, and PTEN-Lin the lung tissue of the EHS groups was significantly higher than in the CON group (Figure 10A) (P <0.001). Compared to the EHS group, the protein levels of Pink1, MFN2, and PTEN-L in the lung tissue of the EHS + Parkin group decreased significantly (P <0.05). There was no significant difference in the expression of Pink1, MFN2, or PTEN-L between the CON + Parkin and CON groups (P >0.05). No significant difference in the expression of PTEN was observed in the lung tissues of any group (P >0.05) (Figure 10B–E).

The immunofluorescence results showed that the fluorescence intensity of Parkin (red) in the lung tissue of the CON + Parkin group was significantly enhanced compared to the CON group (Figure 10F). In the lung tissue of the EHS group, the colocalization (orange) fluorescence intensity of Pink1 (green) and Parkin (red) decreased compared with the CON group. In the EHS + Parkin group, the colocalization fluorescence intensity of Pink1 and Parkin was higher than that of the EHS group. In the CON + Parkin group, the fluorescence intensity of Pink1 did not change compared with CON, whereas the colocalization fluorescence intensity of Pink1 and Parkin was slightly enhanced.

Discussion

HS is a fatal disease caused by heat stress to the body that is characterized by multiple organ failure. HS-induced ALI and ARDS are common complications.[22] We established a rat model of EHS and found that, in an external environment of high temperature and humidity, the core body temperature of rats undergoing high-intensity exercise increased sharply. Significant pathological changes occurred in the lungs, characterized by progressive infiltration of inflammatory cells, massive alveolar hemorrhage, and blurred alveolar structure. These changes led to an increase in the lung coefficient and pulmonary vascular permeability. A large number of apoptotic cells were observed in the lung. This finding is consistent with those

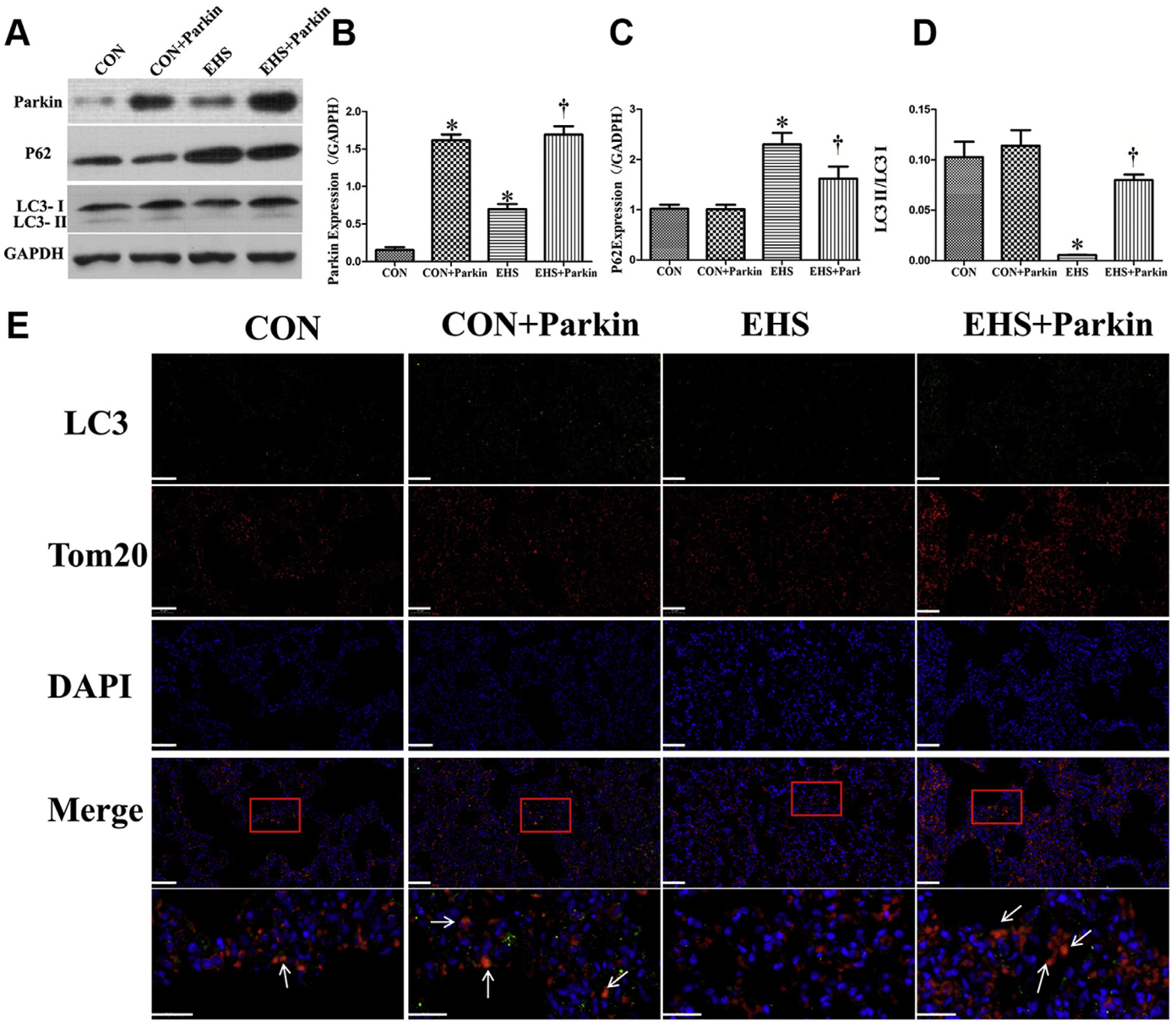

Figure 9. Parkin overexpression rats exhibited an increasing level of mitophagy in the lung. A: Western blotting showing the levels of Parkin, P62, and LC3. B–D: Statistical analysis of Parkin, P62 expression and LC3-I/LC3-II ratio.

*P <0.001 *vs.* CON group;

†P <0.05 *vs.* EHS group.

E: Immunofluorescence staining of LC3 (green) and Tom20 (red). The colocalization (orange) of LC3 and Tom20 is shown by the white arrows. Scale bar = 50 μm.

CON: Control; EHS: Exertional heat stroke; GAPDH: Glyceraldehyde phosphate dehydrogenase; LC3: Light chain 3.

of the previous studies.[5,9,23] The mechanism underlying ALI caused by HS remains unclear. At present, the direct heat injury and the secondary systemic inflammation are believed to be the pathophysiological changes of this disease.[24] Endotoxins and inflammatory cytokines have been detected in the lung tissue during ARDS caused by HS. The inflammatory cell infiltration and alveolar macrophages increased simultaneously, indicating that there was an obvious inflammatory reaction in the lungs of patients with HS.[5] Our study found that in the lung tissue of rats with EHS, the levels of IL-6, IL-1β, and TNF-α were significantly increased, confirming that EHS caused inflammation in these tissues. EHS not only causes local inflammation but also leads to SIRS. Therefore, the immune response of the body is disrupted in EHS, and the cascade amplification of immune cells and inflammatory factors can induce an inflammatory storm, leading to more serious organ and tissue damage.

Oxidative stress plays an important role in the pathological injury caused by EHS. Our results suggest that the level of ROS in the lungs of EHS rats was significantly increased, further confirming that EHS can lead to excessive activation of oxidative stress.

Mitochondrial dysfunction leads to increased intracellular oxidative stress and ROS expression.[25] Transmission electron microscopy showed that the mitochondria in type II lung epithelial cells of rats with EHS were swollen, the mitochondrial

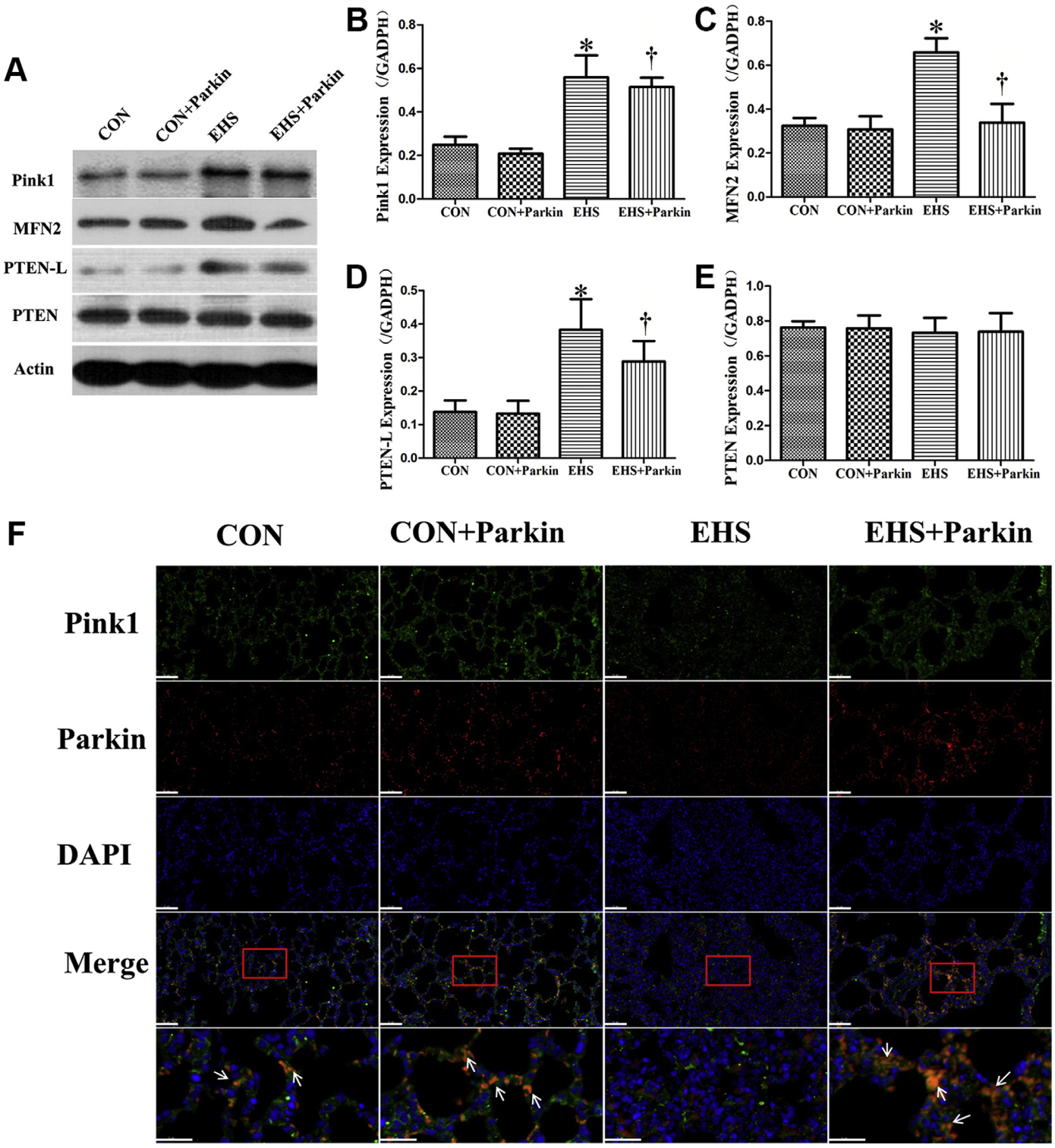

Figure 10. Parkin overexpression activates the Pink1/Parkin pathway in the lungs. A: Western blotting of Pink1, MFN2, PTEN-L, and PTEN. B–E: Statistical analysis of Pink1, MFN2, PTEN-L, and PTEN expression.

*P <0.001 *vs.* CON group;

†P <0.05 *vs.* EHS group.

F: Immunofluorescence staining of Pink1 (green) and Parkin (red). The colocalization (orange) of Pink1 and Parkin is shown by the white arrows. Scale bar = 50 μm.

CON: Control; EHS: Exertional heat stroke; GAPDH: Glyceraldehyde phosphate dehydrogenase; MFN2: Mitofusin-2.

cristae were broken, and most of the mitochondria were vacuolated. The change revealed that the mitochondria in lung tissue cells were seriously damaged by EHS. Injury to mitochondria leads to the accumulation of ROS production, which in turn aggravates mitochondrial damage. This forms a vicious circle, leading to the amplification of ROS, causing a "waterfall" inflammatory reaction, apoptosis, and necrosis of cells; finally progressing to organ failure.[26] Therefore, the timely removal of damaged mitochondria plays a positive role in protecting organ function.

There is a strict quality control system that exists in cells to identify and repair damaged mitochondria and maintain mitochondrial homeostasis. Mitophagy is an important regulatory mechanism that maintains the balance of mitochondrial quantity and quality and preserves the dynamic balance of the intracellular mitochondrial network.[11] Mutations in mitochondrial genes, high intracellular ROS levels, and the chemical factor antimycin may lead to mitochondrial damage and induce mitophagy.[27] Enhanced mitophagy can clear injured mitochondria, reduce oxidative stress response, and alleviate lung injury.[26,27] Our study found that in the lung tissue of rats with EHS, the mitochondria showed swelling, enlargement, disappearance of the mitochondrial crest, and vacuolization. Western blotting showed a decrease in the ratio of LC3-II/LC3-I, a marker of autophagy, and an increase in the expression of p62. Immunofluorescence results showed a reduction in LC3 binding to mitochondria, suggesting a decrease in autophagosomes enclosing the mitochondria. Therefore, the inhibition of mitophagy by EHS may be one of the mechanisms leading to an inflammatory response and cell injury in lung tissue.

Pink1/Parkin-mediated mitophagy is one of the classical pathways. Under the stress of ROS, nutrient deficiency, cell aging, and other effects, the mitochondria in cells will show depolarization of the outer mitochondrial membrane (OMM). Pink1 associates with the OMM and recruits Parkin through autophosphorylation. Activated Parkin polyubiquitinates numerous substrates of OMM proteins, leading to the formation of autophagosomes including the ubiquitin- and LC3-binding receptor SQSTM1/p62.[28,29] Autophagosomes engulf the damaged mitochondria under the guidance of LC3 junction proteins, leading to mitophagy.[29] MFN2 is a downstream molecule in this pathway that inhibits mitochondrial fusion and provides autophagy signals.[30] Pinkl-phosphorylated MFN2 transmits damaged mitochondrial signals to bind to Parkin, while Parkin further ubiquitinates MFN2, thereby recruiting more Parkin and initiating the ubiquitination cycle.[31] Our study showed that although EHS increased the expression of Pink1 and Parkin proteins in rat lung tissue, the degree of binding between them decreased, suggesting that the inhibition of mitophagy by EHS was related to the blockade of the interaction between Pink1 and Parkin. EHS inhibits the activation of the Pink1/Parkin pathway, resulting in a decrease in the production of mitochondrial autophagosomes and the inhibition of mitophagy in the lung tissue. The dysfunction of mitophagy further hinders the degradation of Pink1, Parkin, and MFN2, all of which accumulate in the lung tissue.[32]

PTEN-L is a protein phosphatase that inhibits the phosphorylation of ubiquitin on Ser65 by Pink1, which is a key step in the Pink1-mediated translocation of Parkin to damaged mitochondria and the activation of Parkin E3 ubiquitin ligase. Increased expression of PTEN-L can prevent the translocation of Parkin to the mitochondria, inhibit the E3 ubiquitin ligase activity of Parkin, and prevent Parkin-induced mitophagy.[33] Our study found that the expression of PTEN-L in the lung tissue of EHS rats was increased, whereas PTEN levels did not change. As a negative regulator of the Pink1/Parkin pathway, upregulation of PTEN-L expression can weaken the interaction between Pink1 and Parkin, inhibit mitophagy, and eventually lead to lung injury. This may explain why mitophagy levels decreased, although HS induced an increase in the expression of both Pink1 and Parkin in lung tissues.

Many studies have shown that activating the Pink1/Parkin pathway has a protective effect against lung, kidney, and liver injury caused by sepsis.[13,34,35] In our study, we found that after EHS, the survival rate of rats overexpressing Parkin was significantly better than that of controls. Pulmonary vascular permeability decreased, pathological injury in the lung tissue was alleviated, and pulmonary apoptosis significantly decreased in these animals. The levels of ROS and inflammatory factors IL-6, IL-1β, and TNF-α decreased significantly. Transmission electron microscopy showed that the degree of mitochondrial swelling in pulmonary epithelial cells decreased and no vacuolization was observed. Immunohistochemistry and immunofluorescence showed that Parkin overexpression significantly increased the expression of Parkin in rat lung tissue, enhanced the interaction between Pink1 and Parkin, increased the binding of LC3 to mitochondria, increased the LC3-II/LC3-I ratio, and decreased the expression of p62. These results suggest that Parkin overexpression can partially counteract the inhibition of the Pink1/Parkin pathway by PTEN-L. This promotes mitophagy to clear damaged mitochondria, maintaining the effectiveness of mitochondrial function and cell homeostasis to reduce inflammatory reactions and ROS, alleviates the ALI, and improves the prognosis of EHS rats. In addition, Parkin overexpression reduced the excessive accumulation of Pink1 and MFN2 in the lung tissue after increasing the level of mitophagy. Therefore, the activation of Pink1/Parkin induced-mitophagy has protective effects against the ALI caused by EHS.

A limitation of this study concerns the fact that the Pink1/Parkin pathway is only one of the pathways affecting mitophagy. Proteins on the mitochondrial membrane, such as NIP3-like protein X, can also participate in Parkin-dependent mitophagy.[36] FUN14 domain-containing protein 1 receptor and Bcl-2-like protein 13 induce mitophagy in a Parkin-independent manner.[15,31] Whether these mitochondrial pathways are involved in the pathogenesis of lung injury during HS requires further investigation.

Conclusions

In summary, this study demonstrated that HS could affect the respiratory system and cause lung injuries. Pink1/Parkin-mediated mitophagy dysfunction is one of the mechanisms underlying ALI in rats with EHS, and Parkin overexpression-mediated mitophagy can alleviate ALI caused by EHS.

CRediT Authorship Contribution Statement

Ran Meng: Writing – original draft. **Zhengzhong Sun:** Data curation. **Ruxue Chi:** Data curation. **Yan Gu:** Data curation.

Yuxiang Zhang: Writing – review & editing. **Jiaxing Wang:** Writing – review & editing.

Acknowledgments

None.

Funding

This work was supported by the 2020 Special Tasks for Military Health and Epidemic Prevention and Protection (grant number Hou Wei Han [2021] No. 208) and Hospital Project (grant number 2016ZD-008).

Ethics Statement

The authors assert that all procedures contributing to this work comply with the ethical standards of the relevant national guides on the care and use of laboratory animals and have been approved by the Ethics Committee of the Eighth Medical Center of Chinese PLA General Hospital (approval number: 20208141030). This study is reported in accordance with ARRIVE guidelines.

Conflict of Interest

The authors declare that they have no known competing financial interests or personal relationships that could have appeared to influence the work reported in this paper.

Data availability

The datasets used and/or analyzed during the current study are available from the corresponding author upon reasonable request.

References

[1] The LancetHealth in a world of extreme heat. Lancet 2021;398:641. doi:10.1016/s0140-6736(21)01860-2.
[2] Bouchama A, Abuyassin B, Lehe C, Laitano O, Jay O, O'Connor FG, et al. Classic and exertional heatstroke. Nat Rev Dis Primers 2022;8(1):8. doi:10.1038/s41572-021-00334-6.
[3] Belval LN, Casa DJ, Adams WM, Chiampas GT, Holschen JC, Hosokawa Y, et al. Consensus statement – prehospital care of exertional heat stroke. Prehosp Emerg Care 2018;22(3):392–7. doi:10.1080/10903127.2017.1392666.
[4] Varghese GM, John G, Thomas K, Abraham OC, Mathai D. Predictors of multiorgan dysfunction in heatstroke. Emerg Med J 2005;22(3):185–7. doi:10.1136/emj.2003.009365.
[5] Liu Z, Chen J, Hu L, Li M, Liang M, Chen J, et al. Expression profiles of genes associated with inflammatory responses and oxidative stress in lung after heat stroke. Biosci Rep 2020;40(6):BSR20192048. doi:10.1042/bsr20192048.
[6] Zhang Y, Wang S, Wang X, Zan Q, Yu X, Fan L, et al. Monitoring of the decreased mitochondrial viscosity during heat stroke with a mitochondrial AIE probe. Anal Bioanal Chem 2021;413(14):3823–31. doi:10.1007/s00216-021-03335-2.
[7] Wen Y, Zhang W, Liu T, Huo F, Yin C. Pinpoint diagnostic kit for heat stroke by monitoring lysosomal pH. Anal Chem 2017;89(21):11869–74. doi:10.1021/acs.analchem.7b03612.
[8] Chen Y, Tong H, Pan Z, Jiang D, Zhang X, Qiu J, et al. Xuebijing injection attenuates pulmonary injury by reducing oxidative stress and proinflammatory damage in rats with heat stroke. Exp Ther Med 2017;13(6):3408–16. doi:10.3892/etm.2017.4444.
[9] Wang L, Lu Z, Zhao J, Schank M, Cao D, Dang X, et al. Selective oxidative stress induces dual damage to telomeres and mitochondria in human T cells. Aging Cell 2021;20(12):e13513. doi:10.1111/acel.13513.
[10] Wei H, Liu L, Chen Q. Selective removal of mitochondria via mitophagy: distinct pathways for different mitochondrial stresses. Biochim Biophys Acta 2015;1853(10 Pt B):2784–90. doi:10.1016/j.bbamcr.2015.03.013.
[11] Roca-Portoles A, Tait SWG. Mitochondrial quality control: from molecule to organelle. Cell Mol Life Sci 2021;78(8):3853–66. doi:10.1007/s00018-021-03775-0.
[12] Kang R, Zeng L, Xie Y, Yan Z, Zhou B, Cao L, et al. A novel PINK1- and PARK2-dependent protective neuroimmune pathway in lethal sepsis. Autophagy 2016;12(12):2374–85. doi:10.1080/15548627.2016.1239678.
[13] Chen H, Lin H, Dong B, Wang Y, Yu Y, Xie K. Hydrogen alleviates cell damage and acute lung injury in sepsis via PINK1/Parkin-mediated mitophagy. Inflamm Res 2021;70(8):915–30. doi:10.1007/s00011-021-01481-y.
[14] Kim M, Nikouee A, Sun Y, Zhang QJ, Liu ZP, Zang QS. Evaluation of Parkin in the regulation of myocardial mitochondria-associated membranes and cardiomyopathy during endotoxemia. Front Cell Dev Biol 2022;10:796061. doi:10.3389/fcell.2022.796061.
[15] Zhang Y, Chen L, Luo Y, Wang K, Liu X, Xiao Z, et al. Pink1/Parkin-mediated mitophagy regulated the apoptosis of dendritic cells in sepsis. Inflammation 2022;45(3):1374–87. doi:10.1007/s10753-022-01628-x.
[16] Pan P, Shen M, Yu Z, Ge W, Chen K, Tian M, et al. SARS-CoV-2 N protein promotes NLRP3 inflammasome activation to induce hyperinflammation. Nat Commun 2021;12(1):4664. doi:10.1038/s41467-021-25015-6.
[17] He SX, Li R, Yang HH, Wang ZQ, Peng YM, Huang JH, et al. Optimization of a rhabdomyolysis model in mice with exertional heat stroke mouse model of EHS-rhabdomyolysis. Front Physiol 2020;11:642. doi:10.3389/fphys.2020.00642.
[18] Hong SB, Koh Y, Lee IC, Kim MJ, Kim WS, Kim DS, et al. Induced hypothermia as a new approach to lung rest for the acutely injured lung. Crit Care Med 2005;33(9):2049–55. doi:10.1097/01.ccm.0000178186.37167.53.
[19] Ma C, Dong L, Li M, Cai W. Qidonghuoxue decoction ameliorates pulmonary edema in acute lung injury mice through the upregulation of epithelial sodium channel and aquaporin-1. Evid Based Complement Alternat Med 2020;2020:2492304. doi:10.1155/2020/2492304.
[20] Sendo T, Kataoka Y, Takeda Y, Furuta W, Oishi R. Nitric oxide protects against contrast media-increased pulmonary vascular permeability in rats. Invest Radiol 2000;35(8):472–8. doi:10.1097/00004424-200008000-00003.
[21] Schneider CA, Rasband WS, Eliceiri KW. NIH Image to ImageJ: 25 years of image analysis. Nat Methods 2012;9(7):671–5. doi:10.1038/nmeth.2089.
[22] Liu SY, Song JC, Mao HD, Zhao JB, Song QExpert Group of Heat Stroke Prevention and Treatment of the People's Liberation Army, and People's Liberation Army Professional Committee of Critical Care Medicine. Expert consensus on the diagnosis and treatment of heat stroke in China. Mil Med Res 2020;7(1):1. doi:10.1186/s40779-019-0229-2.
[23] Lin CH, Tsai CC, Chen TH, Chang CP, Yang HH. Oxytocin maintains lung histological and functional integrity to confer protection in heat stroke. Sci Rep 2019;9(1):18390. doi:10.1038/s41598-019-54739-1.
[24] Lim CL. Heat sepsis precedes heat toxicity in the pathophysiology of heat stroke – a new paradigm on an ancient disease. Antioxidants 2018;7(11):149. doi:10.3390/antiox7110149.
[25] Onishi M, Yamano K, Sato M, Matsuda N, Okamoto K. Molecular mechanisms and physiological functions of mitophagy. EMBO J 2021;40(3):e104705. doi:10.15252/embj.2020104705.
[26] Zhao Y, Huang S, Liu J, Wu X, Zhou S, Dai K, et al. Mitophagy contributes to the pathogenesis of inflammatory diseases. Inflammation 2018;41(5):1590–600. doi:10.1007/s10753-018-0835-2.
[27] Yao RQ, Ren C, Xia ZF, Yao YM. Organelle-specific autophagy in inflammatory diseases: a potential therapeutic target underlying the quality control of multiple organelles. Autophagy 2021;17(2):385–401. doi:10.1080/15548627.2020.1725377.
[28] Silvian LF. PINK1/Parkin pathway activation for mitochondrial quality control – which is the best molecular target for therapy? Front Aging Neurosci 2022;14:890823. doi:10.3389/fnagi.2022.890823.
[29] Zhou J, Li XY, Liu YJ, et al. Full-coverage regulations of autophagy by ROS: from induction to maturation. Autophagy 2022;18(6):1240–55. doi:10.1080/15548627.2021.1984656.
[30] McLelland GL, Goiran T, Yi W, Dorval G, Chen CX, Lauinger ND, et al. MFN2 ubiquitination by PINK1/Parkin gates the p97-dependent release of ER from mitochondria to drive mitophagy. Elife 2018;7:e32866. doi:10.7554/eLife.32866.
[31] Fang Q, Zheng S, Chen Q, Chen L, Yang Y, Wang Y, et al. The protective effect of inhibiting mitochondrial fission on the juvenile rat brain following PTZ kindling through inhibiting the BCL2L13/LC3 mitophagy pathway. Metab Brain Dis 2023;38(2):453–66. doi:10.1007/s11011-022-01077-3.
[32] Kawajiri S, Saiki S, Sato S, Sato F, Hatano T, Eguchi H, et al. PINK1 is recruited to mitochondria with Parkin and associates with LC3 in mitophagy. FEBS Lett 2010;584(6):1073–9. doi:10.1016/j.febslet.2010.02.016.
[33] Wang L, Cho YL, Tang Y, Wang J, Park JE, Wu Y, et al. PTEN-L is a novel protein phosphatase for ubiquitin dephosphorylation to inhibit PINK1-Parkin-mediated mitophagy. Cell Res 2018;28(8):787–802. doi:10.1038/s41422-018-0056-0.
[34] Lin Q, Li S, Jiang N, Shao X, Zhang M, Jin H, et al. PINK1-Parkin pathway of mitophagy protects against contrast-induced acute kidney injury via decreasing mitochondrial ROS and NLRP3 inflammasome activation. Redox Biol 2019;26:101254. doi:10.1016/j.redox.2019.101254.
[35] Wang S, Tao J, Chen H, Kandadi MR, Sun M, Xu H, et al. Ablation of Akt2 and AMPKα2 rescues high fat diet-induced obesity and hepatic steatosis through Parkin-mediated mitophagy. Acta Pharm Sin B 2021;11(11):3508–26. doi:10.1016/j.apsb.2021.07.006.
[36] Xu D, Chen P, Wang B, Wang Y, Miao N, Yin F, et al. NIX-mediated mitophagy protects against proteinuria-induced tubular cell apoptosis and renal injury. Am J Physiol Renal Physiol 2019;316(2):F382–95. doi:10.1152/ajprenal.00360.2018.